Near-Room-Temperature Mid-Infrared Quantum Well Photodetector

Sean Hinds, Margaret Buchanan, Richard Dudek, Sofiane Haffouz, Sylvain Laframboise, Zbigniew Wasilewski, and H. C. Liu*

Low-cost mid-infrared (MIR) semiconductor photodetectors that use thermo-electric coolers (TECs) (devices that operate at temperatures above 180K), with high specific detectivities, and with high uniformity over large active areas are not readily available. Presently, mercury-cadmium-telluride is arguably the most important semiconductor alloy system for TEC temperature and high sensitivity infrared detectors; however, this material is expensive and typified by substrate, lattice, surface, and interface instabilities that lead to large (>20%) spatial non-uniformity, and a non-linear responsivity.[1,2] Indium-antimonide detectors are likewise the most important semiconductor material for imaging, by virtue of their lower cost and high spatial uniformity but, typically, at the cost of material fragility, significant 1/f noise, and a need for cryogenic operation to achieve a competitive detectivity. In contrast, quantum well infrared photodetectors (QWIPs) show excellent infrared detection and imaging performance, but have a major limitation to their widespread use: they usually require cooling to cryogenic temperatures. It is therefore critical to develop high performance photodetectors, like QWIPs, that can be operated at room temperature, or at temperatures that can be achieved with TECs. Photovoltaic quantum well infrared photodetectors (PV-QWIPs) enable such devices: low-noise, compact, and robust room temperature devices for hyperspectral imaging, environmental gas sensing, and micro-optoelectronic communications.[3–8] Specifically, InGaAs MIR PV-QWIPs enable innate spectral selectivity, polarization sensitivity, radiation hardness, and high speed operation. In addition, the use of these cost effective mature GaAs based growths allow exceptional material uniformity, reproducibility, and yield, over a large area, which can result in devices with excellent measured detectivities at TEC temperatures without an applied bias.

MIR photoconductive QWIPs operating at temperatures that are accessible by thermo-electric coolers were previously demonstrated; however, their detectivities were inferior to competitive photon and thermal detectors. Those devices would require >10^4 W/cm^2 (10 mW for a 10 μm × 10 μm area device) laser power to operate at room temperature with photon noise limited performance.[9–10] High thermal conductivity indium-phosphide based quantum cascade QWIPs have demonstrated improved performance, but at low background infrared limited performance temperature and, to date, with ill-controlled activation energies.[8,11]

Here, we employ an InGaAs/AlGaAs/GaAs materials approach for 5 μm absorption wavelength photovoltaic design in quantum cascade detector (QCD) low-noise format.[12] We report high signal and noise current measured D* and optoelectronic FTIR responses as a function of temperature–from cryogenic up to room temperatures. We show that these devices, unlike previously reported InP based attempts, possess activation energies commensurate with their optical transition wavelengths, corresponding to ~250 meV. We demonstrate their high background limited infrared performance temperature of ~145K and deduce their respective carrier emission probabilities as a function of temperature. The devices we present offer a unique combination of low-power consumption (zero bias), high uniformity materials, and performance in the 3–5 μm primary infrared atmospheric transmission window at TEC achievable temperatures.[8,10] The monochromatic irradiance needed for photon limited performance is reduced by more than three orders of magnitude, to ~1.65 W/cm^2 (172 μW for a 80 μm x 113 μm area device) at room temperature, for the devices presented here. This improved sensitivity is of importance for many applications, such as gas sensing, where monochromatic light, or a laser, is employed. Finally, we demonstrate a substantive increase in the TEC achievable detectivity to 2.2×10^9 Jones and background limited detectivity to 2.8×10^{10} Jones, for such MIR QWIP detectors.

We posited to increase these devices' high temperature operation by optimizing their free carrier concentration in favor of below-barrier spatial carrier transport via designed optical transition, controlled thermal activation, tunneling, and phonon scattering transport. The uniform free carrier density in QWIPs is often described by its active wells' ground state 2D electron density, which is related to their doping density and Fermi energy.[13] These electrons are scattered in an emission-capture model to result in a 3D mobile carrier contribution above the wells' barriers. Since the Fermi energy affects both absorption quantum efficiency and detectivity via 2D carrier density, we estimated that a relatively high doping density of ~3×10^{18} cm^{-3} is a reasonable choice to balance these traits with high temperature operation. However, higher doping density often correlates

Dr. S. Hinds, Dr. M. Buchanan, R. Dudek, Dr. S. Haffouz, S. Laframboise, Dr. Z. Wasilewski
Institute for Microstructural Sciences
National Research Council Canada
Ottawa, Ontario, K1A 0R6, Canada
E-mail: sean.hinds@nrc-cnrc.gc.ca
Prof. H. Liu
Key Laboratory of Artificial Structures and Quantum Control
Physics Department
Shanghai Jiao Tong University
Shanghai, 200240, China

DOI: 10.1002/adma.201103372

with uncontrolled free carriers unleashed into the barriers of photoconductive QWIPs, which typically result in large dark current noise, and a diminished resistance-area product at zero bias (RoA), where Ro is the device resistance at null bias and A is the mesa area. To lift this limitation we explore the recapture of scattered carriers into auxiliary wells and their preferential photo-assisted spatial transport, for a designed wavelength, via the photovoltaic effect. We demonstrate that the result is sensitive to radiation at the designed wavelength with high responsivity and resistivity at elevated temperatures.

Photovoltaic QWIP approaches improve in their resistivity and detectivity as the capture probability of carriers into the ground state of an active well, and as the emission probability of carriers out of that well, both tend toward unity. In practice, however, the emission probabilities for our present implementations are significantly lower, which impact negatively on our devices' measured performance.

Figure 1a shows a period of our photovoltaic quantum cascade conduction-band structure and its carriers' wavefunctions that were simulated using a numerical Schrödinger equation solver. Gendron et al. originally proposed an architecture from which our structure was derived.[14] The intended carrier transport direction is from left to right in the figure. The active well is n-Si doped with Fermi energy above the lowest eigen-energy state of the whole structure. Its excited state wavefunctions are resonantly coupled to the ground state of the first undoped electron extraction well. Subsequent undoped extraction wells are organized in cascading energies that are separated roughly by the LO phonon energy of the well material, ~35 meV. Resonant tunneling through the thick interface barrier helps maintain high resistivity and good escape probability, while phonon assisted scattering extractions help high-speed operation and help optimize the carrier transit time in the device's responsivity. The arrow in Figure 1a helps identify the escape probability and its intended direction within the structure.

Figure 1b shows the response of one of our QCD devices that was optically coupled using a 45-degree facet to a Bruker IFS 66S FTIR spectrometer. The device shows photodetector response up to room temperature using above kHz modulation. The QCD device room temperature Brewster angle absorption taken from a double-side polished wafer piece was measured to be ~6%: corresponding to a 45-degree facet double pass quantum efficiency of ~62% for the 50 period structures.

Figure 2 illustrates our QCD device's escape/capture carrier probability, shielded and unshielded current density, and RoA performances as a function of temperature.

In a standard analysis for QWIPs, photo-gain is given by g = Pe/N Pc, where Pe is the escape probability from the well, Pc is the capture probability, and N is the number of active well repeats. An optimized PV-QWIP should have both Pe and Pc approaching unity. In the present design Pc near 100% is expected especially at zero or low bias voltages, and we deduce the escape to capture probability ratio by measuring the responsivity of the device to a known input power. Figure 2a shows the device's carrier escape-to-capture ratio for its active wells as a function of temperature, which is resilient to about 190K, and then decreases rapidly from ~40% at 190K to less than 2% at 270 K.

A detector's background limited infrared performance (BLIP) defines a temperature below which noise in the detector is dominated by the noise in the background photon flux, and not the detector's self noise: it is an important condition for extracting the highest sensitivity from a given device. The BLIP temperature here is taken as the temperature for which the device's background photocurrent equals its dark-current. Figure 2b illustrates the device's current/temperature response at zero bias; it reveals a BLIP temperature of ~145 K. Given the illustrated 300K background and dark current densities over temperature, we calculate the incident laser power needed to achieve photon noise limited performance (a device current that is dominated by its photocurrent) to be 172 μW (1.65 W/cm^2) at room temperature, for the implemented 80 μm × 113 μm patterned devices.

When devices are thermal noise limited (above the BLIP temperature) the detectivity, D*, is often estimated from spectral responsivity, temperature, and RoA. In addition, the semiconductor Arrhenius activation energy, the energy that must be overcome in order to initiate carrier transport, can be calculated by measuring RoA as a function of temperature. Figure 2c shows the measured RoA of the designed QCD structure. Previous implementations of QCDs in InP based materials have demonstrated activation energies that appear significantly smaller than the optical transition energy or cut-off wavelength of the detectors.[6,9,14–16] Data presented in Figure 2c indicates that the device presented here possesses an activation energy of ~240 meV: thermal activation of carrier transport is tuned to the detector's intended optical transitions.

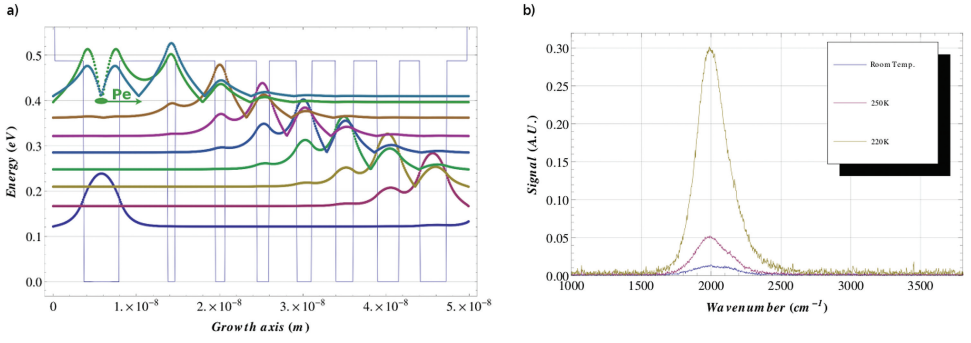

Figure 1. a) Simulated InGaAs/AlGaAs conduction band energy profile, wavefunctions, and escape probability schematic of quantum cascade format. b) FTIR response of quantum cascade device as a function of temperature. The figure enables a direct comparison of the photodetector's theoretical and experimental responses.

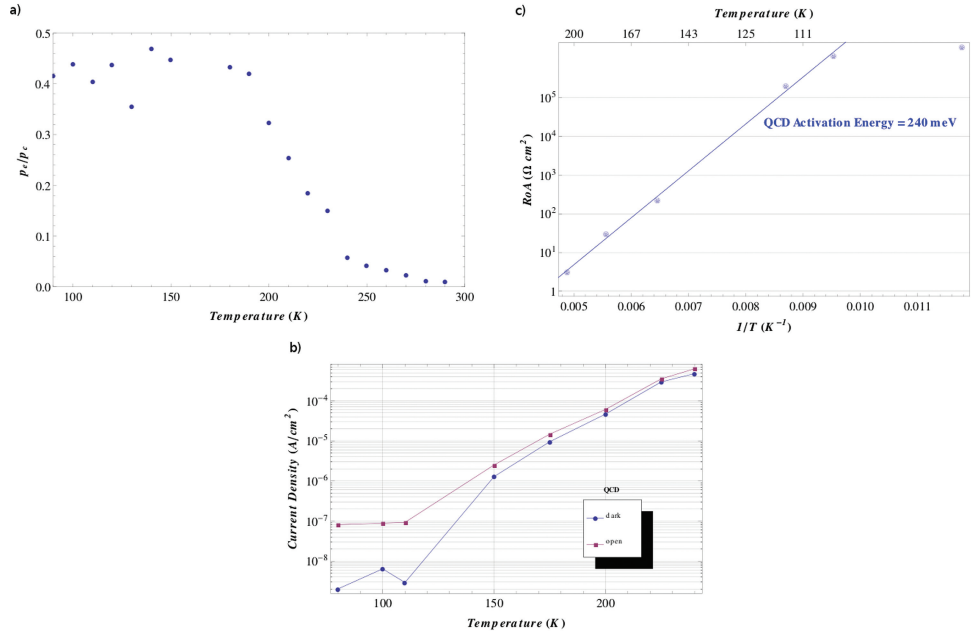

Figure 2. a) Measured escape/capture probability of quantum cascade device over temperature. b) Shielded and 300K background exposure current density of device over temperature. c) RoA of device as a function of device temperature.

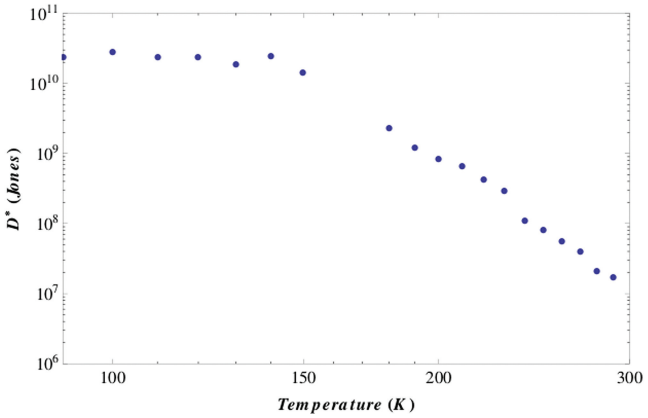

Figure 3. Measured D* as a function of device temperature.

We directly examine the detectivity of the device using the same experimental setup used to measure escape probability by performing input power, current signal, and current signal noise measurements. **Figure 3** illustrates its measured detectivity. The detectivity for the device saturates near 2.8×10^{10} Jones at temperature below ~145 K. The maximum detectivity is observed near 2.2×10^{9} Jones for >180 K (TEC achievable operation). The detector shows an abrupt change in behavior between 140K and 160K, roughly corresponding to a transition from background-limited performance to a thermal-noise-limited performance regime. The background-limited performance should, ideally, give a performance of near 10^{11} Jones implying an improvement of a factor of three could be achieved from these devices with improvements in optical coupling, quantum efficiency, and escape probability.

In summary, we implement a photovoltaic MIR QWIP for room temperature 5 μm absorption wavelength operation using InGaAs/AlGaAs on GaAs materials. We demonstrate a high BLIP temperature of ~145 K, a TEC achievable detectivity of 2.2×10^{9} Jones, and an activation energy that is commensurate with the optical transition design. This work shows that QWIPs which are optimized for room and near room temperature operation may form a viable technology for infrared imaging and sensing.

Experimental Section

Device fabrication: The QCD device active structure consists of 50 periods of a 4.3 nm 12% In(x)Ga(1-x)As 2.8×10^{18} cm^{-3} n-Si doped excitation well along with alternating barriers and wells of: 5.8 nm, 4.8 nm, 3.8 nm, 3.3 nm, 2.9 nm, 2.9 nm, 2.5 nm, 7.6 nm 40% Al(x)Ga(1-x)As barriers, and 0.9 nm, 1.2 nm, 1.5 nm, 1.8 nm, 2.1 nm, 2.6 nm, 3.2 nm 12% In(x)Ga(1-x)As extraction wells. The active region periods are sandwiched between n-Si 1×10^{18} cm^{-3} GaAs contact layers. The device is grown on (100) oriented semi-insulating GaAs substrate by molecular beam epitaxy. Mesas with 180 μm × 255 μm, 120 μm × 170 μm, and 80 μm × 113 μm areas were fabricated using standard photolithography and chemical wet-etching. Ni-Ge-Au ohmic contact metallization was then deposited onto the devices, followed by annealing.

Photoresponse: Devices were mounted in a variable flow liquid nitrogen cryostat fitted with a ZnSe optical window. Light from the FTIR was focused through a 45 degree device facet via a parabolic mirror. Electrical connections to the devices were then fed through a Stanford Research, SR570, pre-amplifier to Bruker analysis software. Responsivity was measured via a 23 Hz chopped 0.1 inch aperture blackbody at 900C through narrow tunable bandpass filters and focused, onto the detectors, via a 4 inch gold parabolic mirror. The input power was verified using a calibrated pyroelectric detector. The output from the pre-amplifier was fed to a Stanford Research 830 lock-in amplifier. Background and thermal limited regimes were measured using a closed cycle Helium cryostat fitted with a variable coldshield and a ZnSe window. We measured the

current-voltage characteristics under dark and near 1.7pi FOV 300K background, open conditions at different device temperatures.

Acknowledgements

H.C.L. was supported in part by the National Basic Research Program of China (Grant 2011CB925603).

Received: September 1, 2011
Published online: November 3, 2011

[1] E. Theocharous, J. Ishii, N. P. Fox, *Infrared Phys. Technol.* **2005**, *46*, 309.
[2] A. Rogalski, *Infrared Phys. Technol.* **1997**, *38*, 295.
[3] S. D. Gunapala, S. V. Bandara, J. K. Liu, C. J. Hill, S. B. Rafol, J. M. Mumolo, J. T. Trinh, M. Z. Tidrow, P. D. LeVan, *Semiconductor Sci. Technol.* **2005**, *20*, 1.
[4] H. Schneider, H. C. Liu, *Quantum Well Infrared Photodetectors Physics and Applications*, Springer, New York United States **2007**, Ch. 8.
[5] H. C. Liu, J. Li, J. R. Thompson, Z. R. Wasilewski, M. Buchanan, J. G. Simmons, *IEEE Electron Device Lett.* **1993**, *14*, 566.
[6] B. Mizaikoff, *Anal. Chem.* **2003**, *75*, 258A.
[7] K. T. Lai, S. K. Haywood, A. H. Mohamed, M. Missous, R. Gupta, *Appl. Phys. Lett.* **2005**, *87*, 192113.
[8] F. R. Giorgetta, E. Baumann, M. Graf, Q. Yang, C. Manz, K. Kohler, H. E. Beere, D. A. Ritchie, E. Linfield, A. G. Davies, Y. Fedoryshyn, H. Jackel, M. Fischer, J. Faist, D. Hofstetter, *IEEE J. Quantum Electron.* **2009**, *45*, 1039.
[9] T. Oogarah, H. C. Liu, E. Dupont, Z. R. Wasilewski, M. Byloos, M. Buchanan, *Semiconductor Sci. Technol.* **2002**, *17*, L41.
[10] Y. F. Lao, P. K. Pitigala, A. G. Perera, H. C. Liu, M. Buchanan, Z. R. Wasilewski, K. K. Choi, P. Wijewarnasuriya, *Appl. Phys. Lett.* **2010**, *97*, 091104.
[11] M. Graf, N. Hoyler, M. Giovannini, J. Faist, D. Hofstetter, *Appl. Phys. Lett.* **2006**, *88*, 241118.
[12] A. Buffaz, A. Gomez, M. Carras, L. Doyennette, V. Berger, *Phys. Rev. B* **2010**, *81*, 075304.
[13] H. C. Liu, R. Dudek, T. Oogarah, P. D. Grant, Z. R. Wasilewski, H. Schneider, S. Steinkogler, M. Walther, P. Koidl, *IEEE Circuits and Devices* **2003**, *19*, 9.
[14] L. Gendron, M. Carras, A. Huynh, V. Ortiz, C. Koeniguer, V. Berger, *Appl. Phys. Lett.* **2004**, *85*, 2824.
[15] F. R. Giorgetta, E. Baumann, M. Graf, L. Ajili, N. Hoyler, M. Giovannini, J. Faist, D. Hofstetter, P. Krötz, G. Sonnabend, *Appl. Phys. Lett.* **2007**, *90*, 231111.
[16] N. Kong, J. Liu, L. Li, F. Liu, L. Wang, Z. Wang, *Chin. Phys. Lett.* **2010**, *27*, 038501.